Indian Journal of Engineering & Materials Sciences
Vol. 30, June 2023, pp. 484-489
DOI: 10.56042/ijems.v30i3.3686

Structural and Optical Properties of Starch-Sodium Alginate Embedded with Cu-Ag Core-Shell Nanoparticles

Navneet Kaur, Jaspreet Kaur, Savita, & Annu Sharma *

Department of Physics, Kurukshetra University, Kurukshetra 136 119, India

Received: 10 May 2023; Accepted: 30 May 2023

In the past few decades, biodegradable polymers obtained from natural resources (such as chitosan, starch, sodium alginate, cellulose, gelatin, etc.) are replacing non-degradable plastics to prevent the further degradation of the environment. Thus, the present study focuses on the synthesis of biodegradable nanocomposites (NCs) using the blend of Starch (St) and Sodium Alginate (SA) as matrix and copper (core)-silver (shell) nanoparticles (NPs) as nanofillers as their distinctive surface plasmon resonance (SPR) band is observed within 350 nm-700 nm *i.e.* in the visible region. For the present study, Cu (core)-Ag (shell) NPs synthesized via a chemical reduction approach were used to fabricate biodegradable Cu-Ag@St-SA NC films via the solution casting technique. The morphological studies of the prepared core-shell NPs were performed using Transmission Electron Microscope (TEM). The size of the Cu-Ag core-shell NPs obtained from TEM comes out to be 18.5±3.0 nm. The NC films were further characterized by UV-Visible spectrophotometer and the data obtained was analyzed to determine Urbach's energy 'E_u', optical energy gap 'E_g', optical conductivity 'σ_{opt}', and refractive index 'n'. The value of 'E_g' for Starch-SA is found to decrease from 4.39 eV to 2.05 eV for 0.48 wt% Cu-Ag@St-SA NC film and 'E_u' increases from 1.04 eV for Starch-SA to 3.03 eV for 0.48 wt% Cu-Ag@St-SA NC film. The NC film containing 0.48 wt% Cu-Ag NPs blocks the UV radiations and thus, can be employed as a UV filter in various devices.

Keywords: Biodegradable, Core-Shell, Optical Energy Gap, Surface Plasmon Resonance (SPR), Urbach's energy

1 Introduction

Bimetallic core-shell nanoparticles (NPs) are the subject of recent studies as they have the potential to combine the properties of two distinct elements into a single nano-entity. Among various metals, noble metallic nanoparticles (NPs) such as copper (Cu) and silver (Ag) are increasingly being investigated as they are strong candidates for potential applications in optical sensors, memory devices, optoelectronic devices, solar cells, etc.[1-3]These NPs show remarkable plasmonic effects such as the appearance of surface plasmon resonance (SPR) band in the visible region and this SPR band can be tuned by varying the size and shape of NPs. Among various metals, NPs of Cu are being studied widely as they have higher conductivity and low cost as compared to other metal NPs.[4] However, the fabrication of Cu NPs is challenging as they are easily oxidized under ambient environmental conditions. Thus, to prevent their oxidation, the Cu NPs are encapsulated under the shell of some other stable metal. The anti-oxidant, anti-resistant, and chemically stable nature of Ag NPs makes them an ideal choice for shell material as Ag shell not only inhibits the oxidation of Cu NPs but also enhances the stability, functionality, and application domain of the NPs.[5]Mallick *et al.*[6] elucidated the stabilization of Cu NPs against oxidation by covering Cu NPs with the shell of Ag NPs and studied their enhanced anti-bactericidal action. Sakt hisabarimoort hi *et al.*[7] also reported the stabilization of Cu NPs by forming a shell of Ag NPs and discussed their non-linear optical applications. Thus, the Cu-Ag core-shell NPs have enhanced physical and chemical properties in comparison to their monometallic NPs. As a result, core-shell NPs have potential applications in widespread fields such as sensing[8,9], optoelectronic devices[10], catalysis[11], inkjet printing[12], etc.

Cu (core)-Ag (shell) nano-scale entities have high surface energy which causes their agglomeration in contrast to their bulk counterparts. Dispersion of these NPs into some appropriate medium is an effective way to resolve this issue. Nowadays, biodegradable polymers are of significant interest as an encapsulating medium because of their low cost, biocompatibility, easy availability, and

*Corresponding author (E-mail:talk2annu@gmail.com)

processability.[13,14] Among various biopolymers, the blend of Sago Starch and Sodium Alginate (St-SA) has been selected as the host matrix due to their remarkable attributes such as hydrophilicity, film forming ability, renewability, non-toxicity, etc. which provide stability to the Cu-Ag NPs.[15,16]

Thus, the current research work focuses on the preparation of Cu-Ag NPs via the chemical reduction method and these NPs were further used to fabricate Cu-Ag@St-SA NC films via a solution casting approach. The fabricated NC films were characterized using Transmission Electron Microscopy (TEM) and their optical properties were determined by using UV-Visible-NIR Spectrophotometer.

2 Materials and Methods

Cu-Ag NPs were prepared in two steps. Firstly, CuNPs were prepared by dissolving 30 mg of $CuSO_4.5H_2O$ and 37.5 mg of starch in 35 ml of deionized water in a round bottom flask for half an hour at 80ºC under continuous stirring. After pouring 1.5 ml of 0.15 M sodium hydroxide into the above mixture, the color of the mixture becomes sky blue. Then, 0.15 ml of hydrazine hydrate was poured into the mixture and the color of the resultant mixture becomes red within a few seconds which indicates the formation of copper (core) NPs. After cooling the solution, 1 ml of 0.07 M $AgNO_3$ was poured into it. The resultant mixture was continuously stirred until its color changed to dark brown indicating towards the formation of Cu (core)-Ag (shell) NPs.

Cu-Ag@St-SA NC films were prepared by mixing 3 g of Sago Starch in 75 ml deionized water at 85°C under vigorous magnetic stirring for 2 hours and the solution was cooled down to 55ºC. Afterward, 3 g of Sodium Alginate (SA) and 0.9 g glycerol (plasticizer) was added to the starch solution and further stirred until a uniform solution was obtained. 0.24 wt% and 0.48 wt% of the prepared colloidal solution of Cu-Ag NPs were added to the St-SA solution and the solution was further stirred for the complete dissolution of NPs. Then, the composite solutions were transferred into Petridishes and dried in an ambient environment (Fig. 1).

The core-shell morphology of the prepared NPs was obtained using Transmission Electron Microscopy (TEM) "Talos" operated at 200 kV. Shimadzu UV-3600 plus UV-VIS-NIR spectrophotometer equipped with an integrating sphere was utilized to determine the optical properties of these NC films.

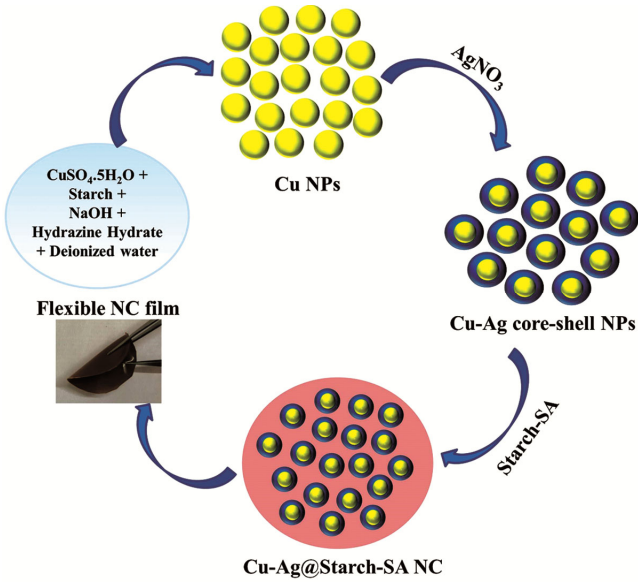

Fig. 1 — Block diagram representing the formation of Cu (core)-Ag (shell) NPs and Cu-Ag@St-SA NC film.

3 Results and Discussion

3.1 Transmission Electron Microscopy (TEM) Analysis

The TEM micrograph of the colloidal Cu (core)-Ag (shell) NPs is shown in Fig. 2. Figure 2 indicates that most of the NPs have a spherical shape and they consist of a lighter outer part and a darker inner part indicating the shell and core parts respectively.[8,17] The average diameter of Cu (core)-Ag (shell) NPs (calculated from Image J software) is about 18.5 ± 3.0 nm. These NPs were further utilized for the fabrication of Cu-Ag@St-SA NC films.

3.2 UV-Visible Absorption Spectra

The UV-Visible absorption spectra of colloidal Cu (core) NPs and Cu (core)-Ag (shell) NPs are presented in Fig. 3(a). The characteristic SPR band originating due to collective oscillations of electrons in the conduction band of Cu NPs appearing at 596 nm indicate towards the formation of Cu (core) NPs while the SPR band appearing at 404 nm (Fig. 3 curve (b)) indicates the formation of Cu (core)-Ag (shell) NPs. Generally, the absorption spectra of bimetallic NPs or alloys contain two distinct SPR bands corresponding to each element but in the case of core-shell NPs, only one band is observed corresponding to shell metal as the core is entirely masked by shell metal.[6,18]

Figure 3 (b) shows UV-Visible-NIR absorption spectra of St-SA and Cu-Ag@St-SA NC films with varying concentrations of Cu (core)-Ag (shell) NPs in St-SA matrix. The absorption spectra of St-SA

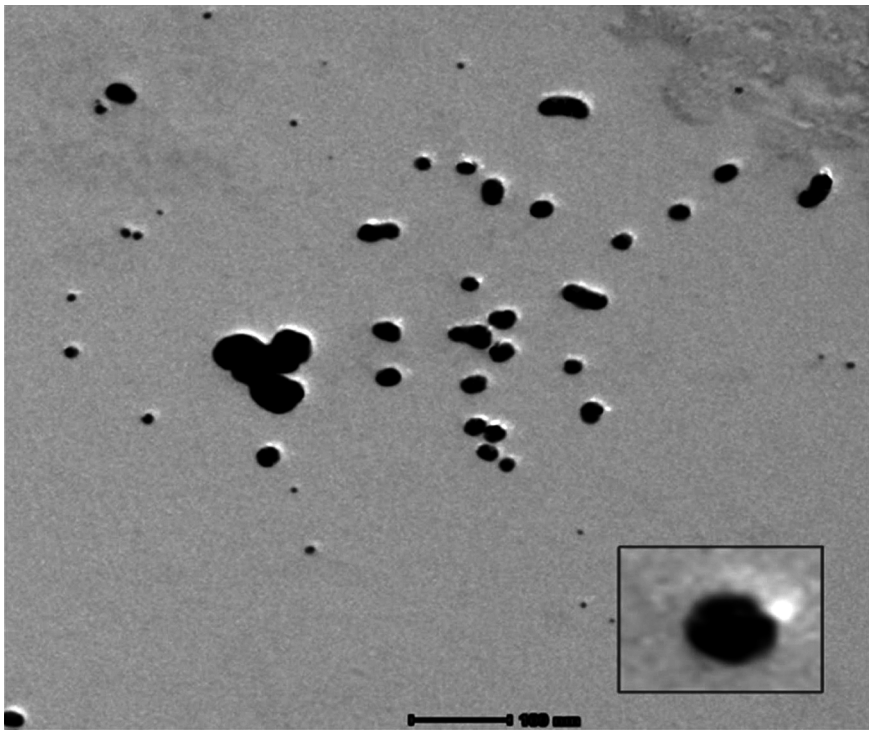

Fig. 2 — TEM micrograph of colloidal Cu-Ag core-shell NPs.

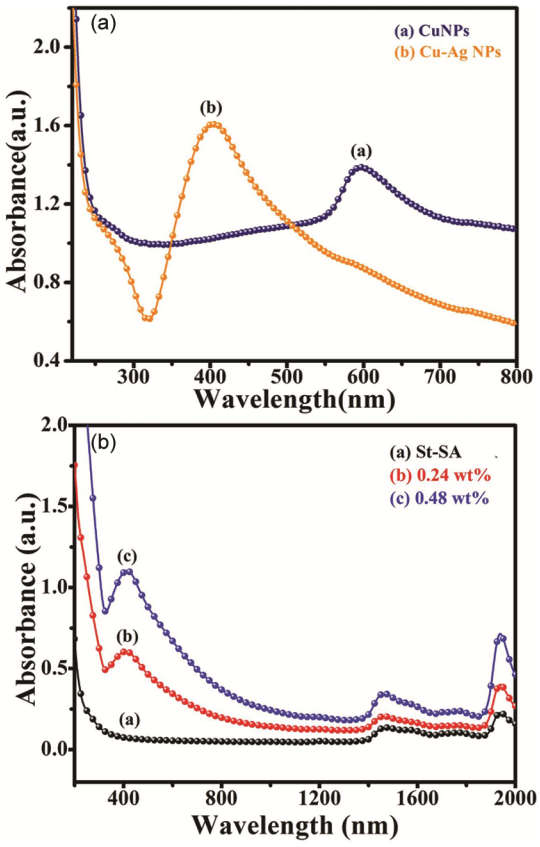

Fig. 3 — UV-Visible absorption spectra of (a) liquid Cu and Cu-Ag NPs, and (b) St-SA and Cu-Ag@St-SA NC films.

consists of a broad band in region 220-255 nm (UV-region) and the visible region, no absorption band is observed. However, the absorption spectra of Cu-Ag@St-SA NC film containing 0.24 wt% Cu-Ag NPs displays SPR band with maxima at ~ 408 nm. This band corresponds to shell material *i.e.* Ag NPs. Further, this SPR band with maxima at ~ 408 nm shifts towards red (~ 416 nm) with increasing content (0.48 wt%) of Cu-Ag NPs. Moreover, the intensity of SPR band increases with increasing concentrations of Cu-Ag NPs in St-SA matrix. This shift as well as an increase in intensity of the SPR band is attributed to the interactions occurring between NPs and polymer blend/change in size, shape, and volume fraction of NPs. [19]Isha *et al.*[20] also reported that with an increase in the concentration of Ag NPs, the SPR band of polyvinyl alcohol-Ag NC gets shifted from 395 nm to 405 nm. These experimental results are in consonance with the theoretical results according to which the position of band maxima gets red-shifted on embedding the Ag NPs in polymer matrices.[21]

3.3 Transmission Spectra

The transmission spectra (UV-Visible region) of St-SA and Cu-Ag@St-SA NC films are presented in Fig. 4(a). It is inferred from the graph that the introduction of Cu-Ag NPs decreases the transmission

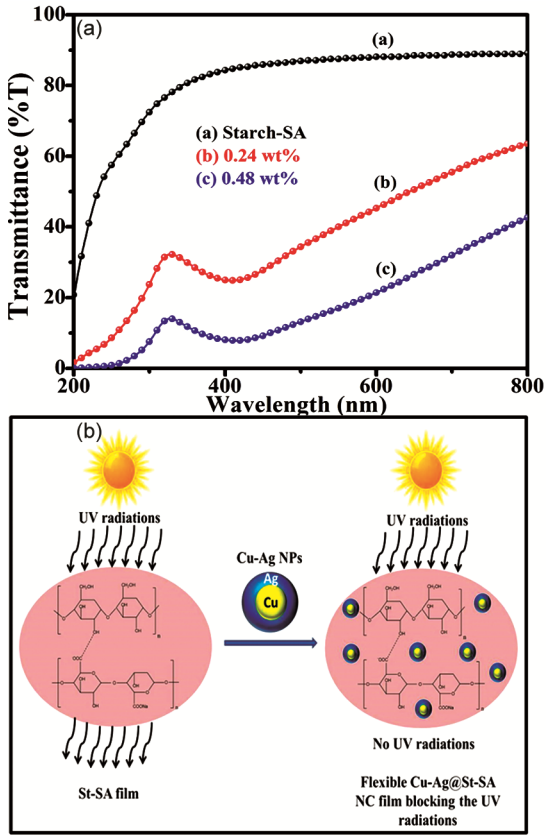

Fig. 4 (a) — Transmission spectra of(a) St-SA, (b) 0.24 wt% and (c) 0.48 wt% Cu-Ag@St-SA NC films and (d) Schematic representation of blocking of UV radiations by Cu-Ag@St-SA NC film.

intensity of St-SA film. The transmission intensity is found to decrease from 6.76% (at 240 nm (UV-region)) for 0.24 wt% NC film to 0.62% for St-SA containing 0.48 wt% Cu-Ag NPs. Thus, these NC films have potential applications for blocking harmful UVradiations (presented in Fig. 4(b)).

3.4 Optical Band Gap 'E_g' and Urbach's Energy 'E_u'

The data obtained from the absorption spectrum of St-SA and Cu-Ag@St-SA NC films was further examined to ascertain the effect of Cu-Ag NPs on various optical parameters *i.e.* optical energy gap 'E_g' and Urbach's energy 'E_u' of St-SA. These optical parameters play a substantial role in deciding the efficacy of using these NC films in several optical devices. For polymeric materials, 'E_g' represents the energy gap between the Highest occupied molecular orbital (HOMO) and Lowest unoccupied molecular orbital (LUMO) and can be computed by utilizing Tauc's law[22,23](equation 1):

$$\alpha h\nu = B(h\nu - E_g)^n \quad \ldots(1)$$

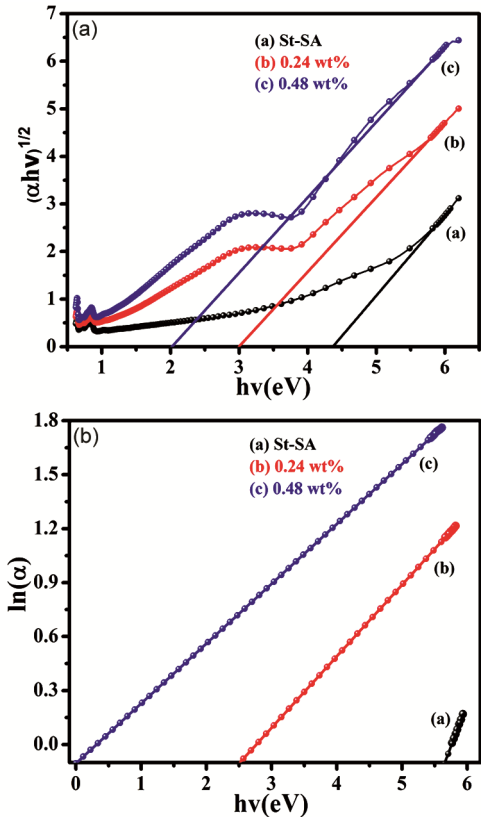

Fig. 5 — (a)'E_g', and (b) 'E_u' for St-SA and Cu-Ag@St-SA NC films.

Here, '$h\nu$' is the energy of the photon, 'B' is a constant depending on transition probability, 'n'characterizes the transition and has different values i.e. 2, 3, 1/2, 3/2 corresponding to allowed indirect, forbidden indirect, allowed direct, forbidden direct transitions respectivelyand 'α'is the absorption coefficient which is computed using the relation 'αd = 2.303 × Absorbance'. Here, 'd' is the thickness of the samples.

The linear fitted curves between $(\alpha h\nu)^{1/2}$and $h\nu$ when extrapolated to $(\alpha h\nu)^{1/2} = 0$ (fig.5(A)) gives the value of indirect energy gap 'E_g'. The calculated values of 'E_g' for St-SA and NC films have been given in Table 1. 'E_g' is found to reduce from 4.39 eV for St-SA to 2.05 eV for 0.48 wt% Cu-Ag@St-SA NC film. The addition of NPs in St-SA matrix introduces interstitial sites within the HOMO-LUMO gap of polymer blend. These interstitial sites increase the probability of lower energy transitions, consequently, 'E_g'decreases[22].The dispersion of Cu-Ag NPs in St-SA matrix produces some disorder in it and this disorder is measured in terms of Urbach's energy (E_u) which can be computed from the relation[24] (equation 2):

Table 1 — 'E_g','E_u', 'n' and 'σ_{opt}' of pristine St-SA and Cu-Ag@St-SA NC films.

Sr. No.	Sample	Optical energy gap (eV)	Urbach's energy (eV)	Refractive Index 'n' (at 416 nm)	Optical Conductivity 'σ_{opt}' (at 416 nm) (ohm^{-1} m^{-1})
1.	St-SA	4.39	1.04	1.96	7.6×10^{6}
2.	0.24 wt% Cu-Ag@St-SA NC	3.02	2.56	1.62	6.5×10^{7}
3.	0.48 wt% Cu-Ag@St-SA NC	2.05	3.03	1.49	9.8×10^{7}

$$\alpha = \alpha_0 exp\frac{h\nu}{E_u} \quad \ldots(2)$$

Here, α_0 is a constant. Urbach's energy has been computed from the linear fitting of $ln(\alpha)$ vs $h\nu$ plot (fig.5(B)) by taking the inverse of the slope. 'E_u'has been found to increase from 1.04 eV for St-SA to 3.03 eV for 0.48 wt% of Cu-Ag@St-SA NC film. This increase is attributed to the defects produced in the polymer blend by the addition of Cu-Ag NPs.

3.5 Refractive Index 'n'

The refractive index 'n' of a material is an important attribute that controls its efficacy to be used in optical devices like filters, switches, and modulators etc. Its value is not constant rather it changes with the wavelength of incident radiations and is determined from extinction coefficient '$k = \alpha\lambda/4\pi$' and reflectance (R) data by utilizing the following relation[22,25] (Equation 3):

$$n = \frac{1+R}{1-R} + \sqrt{\left(\frac{4R}{(1-R)^2}\right) - k^2} \quad \ldots(3)$$

The variation of 'n' with wavelength for pristine St-SA and Cu-Ag@St-SA NC film is depicted in fig. 6(A). The value of 'n' decreases from 1.96 (at 416 nm) for St-SA to 1.62 and 1.49 for 0.24 wt% and 0.48 wt% Cu-Ag@St-SA NC films respectively. Abdelhamied *et al.*[26] also observed a decrease in the refractive index of polymer blend (polyvinyl alcohol/polyaniline) with the incorporation of Ag NPs and attributed this decrease to the increased density as well as strain in the films. Thus, the addition of Cu-Ag NPs in St-SA matrix also increases the density of the films; as a result, 'n' decreases.

3.6 Optical Conductivity 'σ_{opt}'

The drifting of charge carriers in the material under the effect of electric components of the incident electromagnetic radiations is termed as optical conductivity 'σ_{opt}' and is a measure of the rate of absorption of incident energy by the material under investigation. It is calculated from the values of refractive index 'n' and absorption coefficient 'α' using relation[24](equation 4):

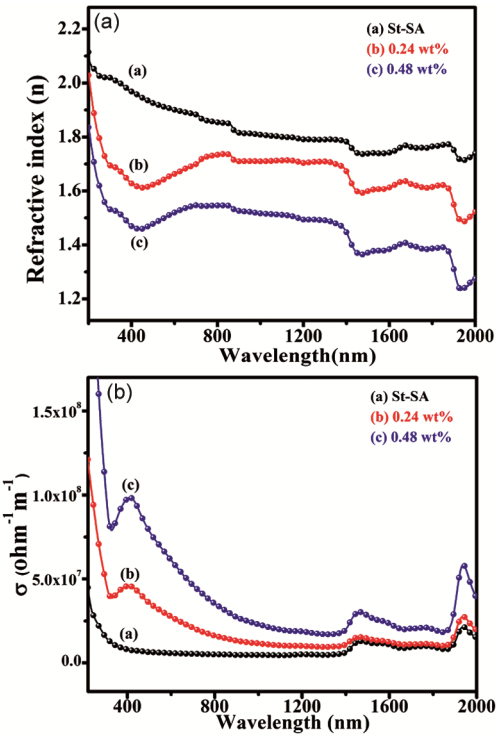

Fig. 6 — The behavior of (a) refractive index 'n' with wavelength and (b)'σ_{opt}' vs wavelength for pristine St-SA and Cu-Ag@St-SA NC films.

$$\sigma_{opt} = \frac{n\alpha c}{4\pi} \quad \ldots(4)$$

Here, 'c' is the speed of light.

The behavior of 'σ_{opt}' with variation in the wavelength of incident radiations is shown in fig. 6(B). It is discerned from the graph that the value of 'σ_{opt}' increases with increasing content of nanofillers in St-SA matrix (given in Table 1). This might be due to the appearance of new interstitial sites within the HOMO-LUMO gap of the polymer blend with the addition of NPs. These interstitial sites enhance the feasibility of low-energy transitions; thus, increasing the rate of absorption of incident radiations. These results are also supported by the results of 'E_g'.

4 Conclusions

The current research work reports the preparation of Cu (core)-Ag (shell) NPs via a chemical reduction approach and subsequently, Cu-Ag@St-SA NC films

via a solution casting approach. TEM ascertained the core-shell structure of prepared NPs. The appearance of SPR band at 404 nm in UV-Visible absorption spectra of Cu-Ag NPs further confirms that Cu (core) is masked by Ag (shell) as it contains no SPR band related to Cu NPs. The absorption and reflectance data obtained from UV-Vis-NIR spectroscopy was further used to determine various optical parameters. It can be inferred from the results that the insertion of Cu-Ag NPs in St-SA matrix introduces some interstitial sites in the HOMO-LUMO gap of the polymer blend which enhances the feasibility of lower energy transitions and leads to a reduction in 'E_g' and increase in 'E_u' and 'σ_{opt}'. Moreover, the NC film containing 0.48 wt% Cu-Ag NPs blocks the incoming UV-radiations to large extent and thus, can be used as a UV-filters. The obtained optical results make these NC films a favorable choice for their potential applications in optoelectronic devices.

Acknowledgment

One of the authors, Navneet Kaur would like to thank CSIR-UGC, New Delhi, India for providing a UGC-SRF fellowship to carry out research work.The authors are also thankful to Department of Science & Technology (DST) for providing UV-Visible-NIR spectroscopy available at Ion Beam Centre, Kurukshetra University, Kurukshetra.

References

1 V P Prakashan, G George, M S Sanu, M S Sajna, A C Saritha, C Sudarsana kumar & N V Unnikrishnan, *Appl Surf Sci*, 507 (2020)144957.
2 M Kang, K J Baeg, D Khim, Y Y Noh & D Y Kim, *Adv Funct Mater*, 23(28) (2013) 3503 .
3 A Zada, P Muhammad, W Ahmad, Z Hussain, S Ali, M Khan & M Maqbool, *Adv Funct Mater*, 30(7) (2020) 1906744.
4 S Shang, A Kunwar, Y Wang, X Qi, H Ma & Y Wang, *Appl Phys A*, 124(7) (2018) 1.
5 C K Kim, G J Lee, M K Lee & C K Rhee, *Powder Technol*, 263 (2014) 1.
6 S Mallick, P Sanpui, S S Ghosh, A Chattopadhyay & A Paul, *RSC Adv*, 5(16) (2015) 12268.
7 A Sakthisabarimoorthi, M Jose, SA Martin Britto Dhas & S Jerome Das, *J Mater Sci Mater Electron*, 28(6) (2017) 4545.
8 R Kumar, R Kaushik, R Kumar, DA Jose, PK Sharma & A Sharma, *Mater Chem Phy*, 260 (2021) 124132.
9 K Shrivas, S Patel, SS Thakur & R Shankar, *Lab on a Chip*, 20(21) (2020) 3996.
10 DH Jiang, PC Tsai, C C Kuo, FC Jhuang, HC Guo, SP Chen & SH Tung, *ACS Appl Mater Interfaces*, 11(10) (2019) 10118.
11 M Ismail, MI Khan, SB Khan, MA Khan, K Akhtar &AM Asiri, *J MolLiq*, 260 (2018) 78.
12 X Yu, J Li, T Shi, C Cheng, G Liao, J Fan & Z Tang, *J Alloys Compd*724 (2017) 365.
13 H Liu, R Jian, H Chen, X Tian, C Sun, J Zhu & C Wang, *Nanomaterials*, 9(7) (2019) 950 .
14 I Armentano, D Puglia, F Luzi, CR Arciola, F Morena, S Martino & L Torre, *Mater*, 11(5) (2018) 795.
15 TM Swamy, B Ramaraj& J H Lee, *J Appl PolymSci*, 109(6) (2008) 4075.
16 ZW Abdullah & Y Dong, *J Mater Sci*, 53(22) (2018) 15319.
17 J Zhao, D Zhang & J Zhao, *J Solid State Chem*, 184(9) (2011) 2339.
18 SF Sabira, AM Kasabe, PC Mane, RD Chaudhari& PV Adhyapak, *Nanotechnol*, 31(48) (2020) 485705.
19 S Venkatachalam, Ultraviolet and visible spectroscopy studies of nanofillers and their polymer nanocomposites, *Spectroscopy of polymer nanocomposites*, (2016) 130
20 I Saini, J Rozra, N Chandak, S Aggarwal, PK Sharma & A Sharma, *Mater ChemPhys*, 139(2-3) (2013) 802
21 A Slistan-Grijalva, R Herrera-Urbina, JF Rivas-Silva, M Ávalos-Borja, FF Castillón-Barraza & A Posada-Amarillas, *Physica E: Low-dimensSystNanostruct*, 27(1-2) (2005) 104
22 Sonal, A Sharma & S Aggarwal, *Opt Mater*, 84 (2018) 807.
23 HK Kaushik, S Kumar, MG Chaudhary & S Khan, Indian J Pure ApplPhys, 58 (2020) 11.
24 Durgesh, R Kumar, PK Sharma & A Sharma, *Mater Sci Eng B*, 276 (2022) 115560.
25 V Bhavsar& D Tripathi, Indian J Pure ApplPhys, 54 (2016) 105.
26 MMAbdelhamied, A Atta, AM Abdelreheem, ATM Farag& MM El Okr, *J Mater Sci: Mater Electron*, 31(24) (2020) 22629.